Time, space and spectrally resolved photochemistry from ensembles to single molecules

F.C. De Schryver

Departement. of Chemistry K.U.Leuven
Celestijnenlaan 200F
B-3001 Heverlee Belgium
Belgium
Frans.deschryver@chem.kuleuven.ac.be

Abstract : Coupling of photophysical and photochemical techniques to microscopy eventually assisted by manipulating techniques, such as laser trapping, has facilitated obtaining information on heterogeneous organic and bio-organic systems by mapping their optical and excited state properties. Scanning confocal microscopy, eventually of laser trapped ensembles, coupled to fluorescence decay analysis and imaging, scanning plate confocal and scanning near field optical microscopy provide combined spectral and spatial resolution down to a few tenths of nanometers. An even better resolution can be achieved using scanning tunneling microscopy. In this contribution a number of organic and macromolecular systems are discussed first in solution and in a next step assembled either in a trap or at a surface. The techniques are illustrated and their limits assessed using latex particles labeled with fluorophores. Time resolved spectroscopy in solution allows the evaluation of migration of the excited state and the collapse of the arms in a dendritic structure. These and other macromolecular structures can be trapped and the obtained assembly visualized and analyzed. Deposition by self-assembly provides the possibility using scanning near field optical microscopy to investigate the excited state properties of ordered arrays. By dilution in a polymer film of dendritic structures single particle, single chromophore and single molecule spectroscopy becomes accessible. Scanning tunneling microscopy is successfully applied to illustrate the visualization and manipulation of structures with subnanometer resolution and the study of their properties including stimulus by light induced transformations.

INTRODUCTION

One of the most fascinating developments in chemistry is the recent technical possibility to visualize particles, molecules and even beyond using different scanning microscopies. On the other hand can time resolution be extended down to a few femtoseconds. The combination of limits in space and time resolution together with photochemistry, photophysics and femtoseconds spectroscopy has been a goal within our research group over the last four years. This report, at the occasion of the Porter Award, is a diary of the enchanted places this voyage has taken me and a group of extremely enthusiastic coworkers. It certainly does not properly honor all the other scientist active in part of the areas mentioned but proper references to them can be found in the original articles cited. In the first part solution photophysics will be used to investigate how chromophores interact or how photophysics can report on solution dynamics. In a second part these methodologies will be coupled to spatial resolution and properties of excited state from supramolecular ensembles of molecules to a single macromolecule will be investigated. In the last part submolecularly resolved imaging of photoactive mono ad-layers on graphite will be discussed.

RESULTS and DISCUSSION

Time resolved spectroscopy in solution.

Time resolved fluorescence decay analysis together with *fluorescence depolarization* allows the study of intramolecular excitation energy migration. The site-to-site intramolecular excitation transfer and excitation trapping on one site in amino-substituted triphenylbenzene derivatives represented in figure 1, which are characterized by a threefold symmetry, have been studied by *fluorescence spectroscopy and time-resolved microwave conductivity* (TRMC). (1). The interpretation of the experimental results is based on the comparison of the molecules with C_3-symmetry with biphenyl model compounds. The localized character of the polar excited state of amino-substituted triphenylbenzene derivatives with threefold symmetry has been studied. The similar absorption and emission properties of the symmetric compounds and the model compounds indicate that the excited state reached immediately after excitation and vibrational relaxation, is localized in one branch of the threefold symmetric compound. During the lifetime of the excited state, however, intramolecular excitation transfer occurs between three energetically degenerate excited states.
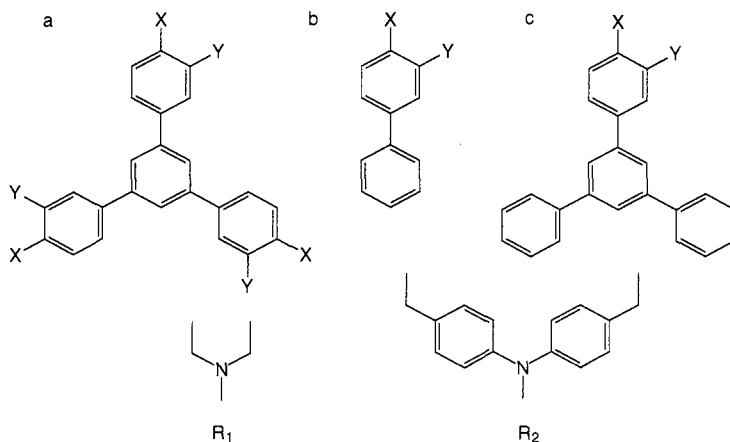

Figure 1. Structures of a) the triphenylbenzene compounds pETP (X=R$_1$, Y=H), mETP (X=H, Y=R$_1$), pEFTP (X=R$_2$, Y=H) and mEFTP (X=H, Y=R$_2$), b) the biphenyl model compounds mEBP (X=H, Y=R$_1$), pEFBP (X=R$_2$, Y=H) and mEFBP (X=H, Y=R$_2$) and c) 1-pETP (X=R$_1$, Y=H).

This redistribution of transition dipoles will depolarize the emission to a certain extent. Hence the limiting anisotropy of mETP is smaller than 0.4 which has been observed for the model compound mEBP and indicates collinear transition dipoles for the latter compound. Due to this flip-flop mechanism, the relaxation of the dipole involves beside the rotational diffusion an intramolecular relaxation path. The importance of this process has been demonstrated in the analysis of the TRMC transients where it is necessary to obtain a similar excited state dipole moment for the triphenylbenzene and its model compound consistent with the solvatochromic shift of the emission.

If the exciton would be redistributed completely among the three sites during the lifetime of the excited state, the limiting anisotropy, however, would be 0.1. The larger value experimentally obtained for mETP suggests that the flip-flop between different sites in 1,2-propanediol at -60 °C is slow with respect to the other deactivation processes of S$_1$. This is probably due to a relative small interaction between the three branches. Moreover, in a rigid glass matrix, the three sites will be stabilized to a different extent in the polar excited state so that the degeneracy disappears. This is translated in an increase of the limiting anisotropy when excitation occurs in the red-edge of the absorption band. The exciton will be trapped in the most stable site from where emission mainly will occur. For pEFTP in benzene at room temperature the limiting anisotropy is close to 0.1 and suggests a fast intramolecular excitation transfer compared to the excited state lifetime.

Upon excitation, a relative large increase of the polarizability, which consists of an electronic and dipolar contribution, is observed for all compounds. While for the model compounds the dipolar contribution

is negligible, the large dipolar contribution for the symmetric compounds indicates an intramolecular excitation transfer in the time range of the reciprocal radian frequency ω. The dipole relaxation time associated with the latter process has been estimated to approximately 10, 73, 4 and 27 ps for pEFTP, mEFTP, pETP and mETP respectively. The meta or para substitution pattern, as well as the molecular geometry of the molecule and the solvent reorganization around the branches influence the interaction between the three amino-sites and hence determine the rate of intramolecular excitation transfer.

R = C6H5 or C6H4C16H33
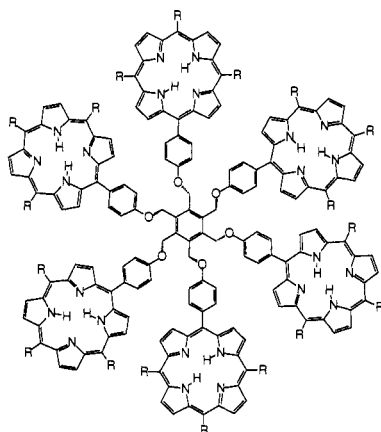
Figure 2. Hexaporphyrinbenzene

Femtosecond transient spectroscopy (2) is an alternative method to study excitation delocalization if the transfer process becomes much faster. Femtosecond transient absorption measurements have been carried out on a hexaporphyrinbenzene BP$_6$ (Figure 2), and on the porphyrin monomer model (BP$_1$). Both were excited at 650 nm (magic angle configuration, 100 μW), while the probe wavelength was in the range of 560 nm to 685 nm (0.7 μW). For both compounds probing below 650 nm a positive signal was recorded which could be assigned to the excited state absorption, whereas at longer wavelengths the ground state bleaching has been observed (figure 3).
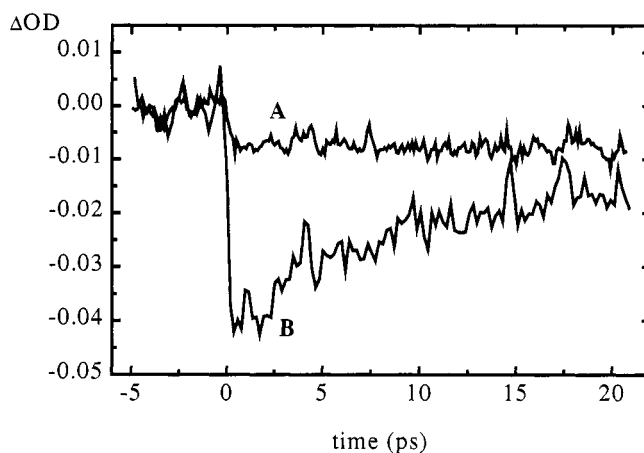
Figure 3. Femtosecond transient absorption decays of BP$_6$ (A) and BP$_1$ (B) in CHCl$_3$ solutions recorded exciting at 650 nm and probing at 670 nm using linearly polarized light in parallel configuration.

Analysis of the data revealed that the signal amplitude for BP_6 is generally smaller than for the monomer under the same experimental conditions indicating a difference in the photophysical behavior of the hexamer and the model, which could be related to the porphyrin interaction. The kinetic recovery of the bleaching showed a clear polarization dependent component for the model compound, while for the hexamer no such component could be detected, suggesting a fast depolarization in the cyclic array.

Fluorescence decay analysis not only reports on processes related to the chromophores as such but can also reveal information on the interaction between the molecules and the solvent even if there is no effect of polarity or polarization. Four generations of a dendrimer (figure 4) with a fluorescent core consisting of a rubicene moiety (3) are synthesized. The biexponential nature of fluorescence decay in toluene indicates the presence of two emitting conformations. Molecular modeling suggests that a conformation where the dendrons interact with the core is not improbable.
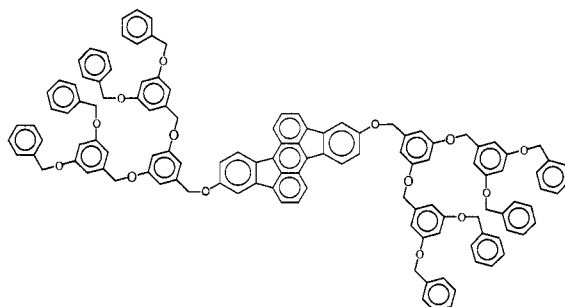

Figure 4. Dendritic structure with a rubicene chromophore core Rb_3.

The relative weight of the two decay times indicates that the contribution of that conformation in toluene increases as the dendrimer generation increases. In acetone and acetonitrile however the fluorescence decay is, except for the fourth generation, monoexponential. The hydrodynamical volume of the dendrimer is determined in toluene, a good solvent, acetone, a medium quality solvent and acetonitrile, a poor solvent with the time resolved fluorescence depolarization technique. No change of the hydrodynamical volume is found in toluene in a temperature range between 20°C and 94°C. (table 1)

Table 1 Van der Waals volume (V_{VDW}), hydrodynamical volume of Rb_n in toluene at different temperatures, the averaged hydrodynamical volume (V_{av}), and free volume (V_{free}.)

	MW^{α} g/mol	V_{VDW} $Å^3$	$V_{21°c}$ $Å^3$	$V_{50°c}$ $Å^3$	$V_{75°c}$ $Å^3$	$V_{94°c}$ $Å^3$	V_{av} $Å^3$	V_{free} $Å^3$
Rb_1	962	875	4030	3540	4070	3740	3850/250	2900
Rb_2	1810	1619	7710	7290	8300	7530	7700/400	6100
Rb_3	3506	3107	12500	12497	13100	12900	12700/300	9600
Rb_4	6898	6083	18800	18850		21100	19600/1300	13600

$^{\alpha}$ molecular weight

Table 2: Fluorescence decay parameters, $V_{hydr.}$, V_{free} and solubility of Rb_n in ACN at room temperature.

	τ (ns)	β	ϕ (ns)	χ^2	$V_{hydr}{}^b$ $(Å^3)$	V_{free} $(Å^3)$
Rb_1	2.76	0.34	0.29	1.09	3230	2360
Rb_2	2.81	0.35	0.60	1.12	6590	4970
Rb_3	3.10	0.33	0.88	1.15	9730	6620
$Rb_4{}^a$	2.43 (0.69) 4.11 (0.31)	0.21	0.59	1.10	6490	407

^{a} biexponential model is necessary to satisfactorily describe the fluorescence decay, the relative contributions of both decay times is indicated in brackets. τ decay time, ϕ rotational correlation time
^{b} assuming a viscosity of 0.36 mPas

This suggests that the dendrimers of all the generations are fully expanded in this solvent. In acetonitrile (table 2) however the hydrodynamical volume of the dendrimers is substantially smaller than in toluene and acetone. This effect is most clear for the fourth generation dendrimer. For this compound the hydrodynamical volume is only a few percentages larger than the excluded volume. Calculation of the molar density, $\rho = MW/V_h \times N_A$, confirms that the dendrimer becomes more and more dense as it increases in generation and that free volume is extremely reduced when the quality of the solvent decreases (figure 5).
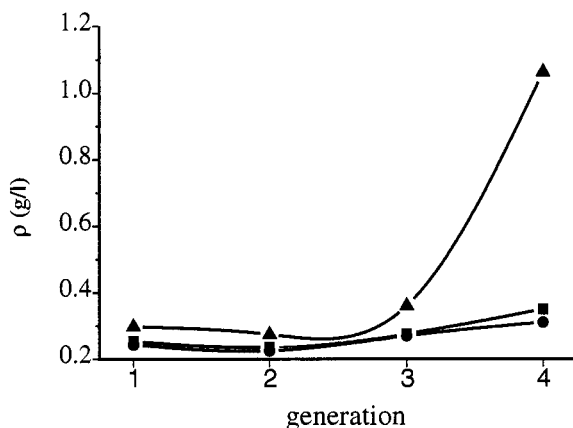

Figure 5. Plot of the molecular density (ρ) as a function of generation; in toluene (■), in acetone (●) and in ACN (▲).

Fluorescence Analysis and Imaging in a laser trap.

Confocal Fluorescence Scanning Microscopy (CFSM) with fluorescence imaging has, theoretically, a spatial resolution approaching $0.6\lambda/NA\sqrt{2}$ (*NA* stands for the numerical aperture) in the lateral and $1.4n\lambda/NA^2$ (*n* is the refractive index) in the axial direction (4). *Optical trapping*, a technique pioneered by Ashkin (5,6) is based on the momentum conservation in interactions of photons with molecules (7). It is established by the radiation pressure exerted by an electronically non-resonant light beam, focused into a solution through a high magnification lens with large numerical aperture. The optically trapped particles, forming a cluster, can be of a very different nature (8). Optical trapping can be combined with transmission microscopy (TM), confocal and non-confocal fluorescence scanning microscopy (CFSM and FSM, respectively), and confocal and non-confocal time-resolved fluorescence spectroscopy (CTRFS and TRFS, respectively) to study latex particles and block copolymer micelles (9).

Dye-labelled latex particles of various size, in polymer composite films as well as optically trapped in solution, were studied with CFSM to characterise the limits of the set-up. CFSM revealed that the resolution in the x- and y-direction was near to the theoretical limit, i.e., 200-250 nm. CTRFS on the labelled latex particles revealed that the decay time of the label was not influenced by the polymer matrix, nor the optical trap.

Poly(*tert*-butylstyrene-*block*-sodium methacrylate) micelles (diameter approximately 30-40 nm) in deuterated aqueous solutions could be optically trapped, this region of high copolymer micelle concentration are referred to as a trapped cluster. In the transmission images, trapped clusters of 1.5-2 μm diameter were detected(figure 6a). Fluorescence images were obtained using perylene as a fluorophore that is specifically dissolved within the block copolymer micelles(figure 6b).

The size of the trapped cluster, estimated from TM and FSM images, increases with increasing irradiation time and power, respectively. In the TM images, the trapped cluster appears as a dark spot (low transmission) with a bright (high transmission) corona-like ring around it. Taking the corona into account when calculating the diameter of the trapped clusters, a very good agreement is found between TM and FSM.

With CFSM it could be shown that the trapped particle has a spot size of approximately 1.7 μm in the region of the IR laser focus, while the diameter extends up to 5 μm without using the confocal imaging capability. The reason for this is that the conditions for optical trapping are fulfilled not only in, but also above and below, the focal region. Due to the high numerical aperture, a dump-bell like shape of the trapped cluster results.
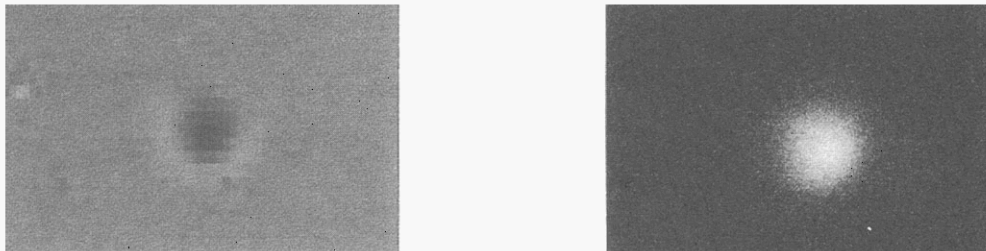
Figure 6.TM (a) and FSM images (b) respectively of the cluster formed by tBSM in the optical trap (trap power P_{1064} = 220 mW, trap time t_{trap} = 120 s).

Fluorescence Analysis of self assembled organic mesoscopic structures on surfaces.

We recently reported a detailed investigation of the local optical properties of porphyrin rings on glass. The ring shaped assemblies on glass were analogous to those previously reported on graphite surfaces, ranging from 10 nm to 10 μm in diameter and 10-200 nm in height. Emission spectra of the rings on the glass indicated that the rings are composed of porphyrin molecules in a locally aggregated configuration (10).
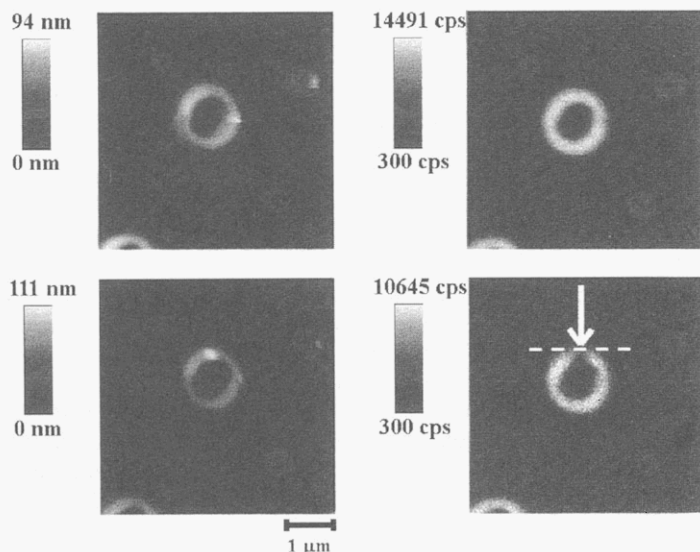
Figure 7 (top left A-to bottom right D) NSOM topography and fluorescence images taken on a sample prepared by solvent casting of a 10^{-6} M solution of BP_6 in $CHCl_3$. (A) Topography and (B) simultaneously acquired fluorescence image taken before bleaching. (C) Topography and (D) fluorescence image from the same region of the sample taken after bleaching. $\lambda_{exc.}$ = 514 nm. The black scale bar below image (C) applies for all images .

Polarized NSOM images further demonstrated that the individual aggregates in the rings are randomly oriented leading to an amorphous conglomerate of nanometer scale aggregates. A model for the mechanism of ring formation has recently been formulated (11) and this phenomenon has been extended to Hexaporphyrinbenzene BP₆ (figure 2)

NSOM topography and fluorescence images were taken on a sample prepared by solvent casting of a 10^{-6} M solution of BP_6 in $CHCl_3$ (figure 7). Topography and simultaneously acquired fluorescence images were taken before bleaching. Positioning the NSOM probe and irradiating the sample during 20 min at the position indicated performs bleaching. Topography and fluorescence images from the same region of the sample taken after bleaching. $\lambda_{exc.} = 514$ nm were taken. From the line scan of the intensity (figure 8) before and after bleaching it clear that a permanent "intensity hole" could be created with a width of approximtely150 nm.
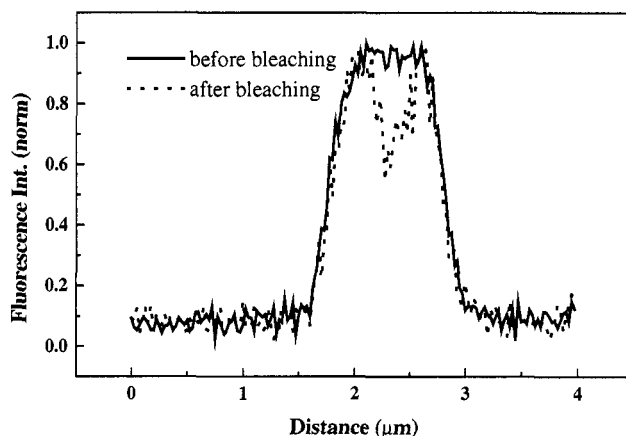

Figure 8. Line profiles of intensities taken at the position of the dashed line indicated in figure 7D before and after the bleaching experiment

Fluorescence imaging of a single macromolecule .

Three generations of dendrimers with a fluorescent core were synthesized by attaching dendrons of the Fréchet type to a Dihydropyrrolopyrroledione (figure 9 DPP₃) molecule.
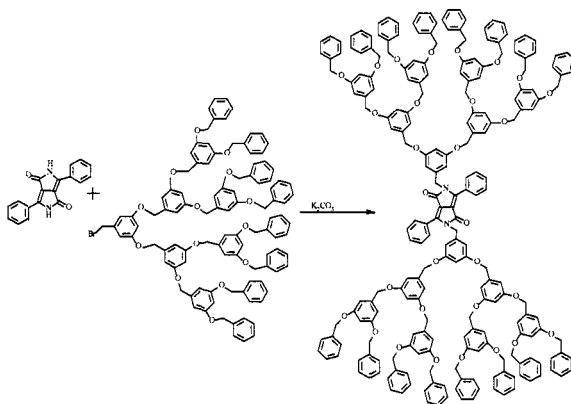

figure 9. Dihydrpyrrolopyrrole based dendritic structures

Samples were prepared by spincoating a toluene solution containing 2×10^{-9} M of the dendrimers and 3mg/ml polystyrene (MW 45000) on a glass cover slip. By exciting near the absorption maximum of the chromophore in the dendrimer, single dendrimer molecules could be imaged via a *plate scanning confocal microscope*. (figure 10A)
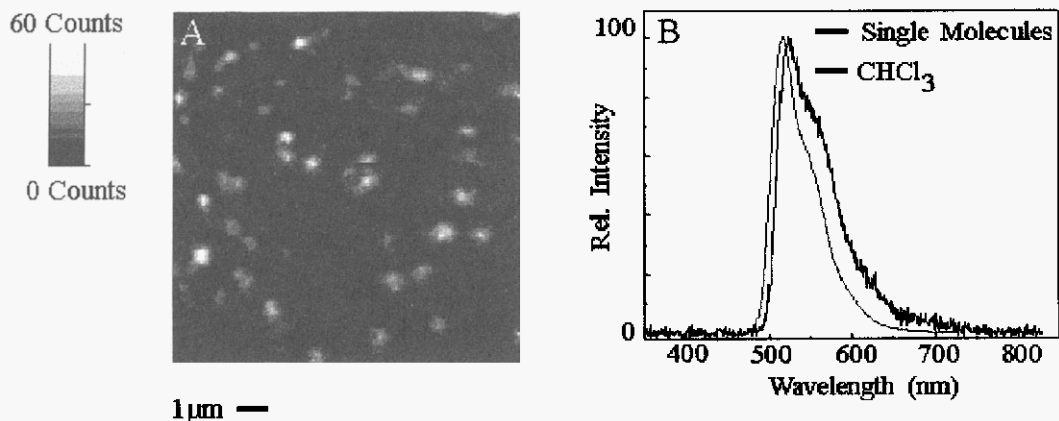

Figure 10. A. A 10 μm by 10 μm image of a thin polystyrene film containing 10^{-9} M on DPP$_3$ dendrimer. B. Spectrum obtained by averaging 20 spectra recorded from bright dots in A compared with a solution spectrum of DPP$_3$

A typical example of scanning an area of a sample containing dendrimers is shown in figure 10A. All the bright spots represent fluorescence signals of single dendrimers or of small clusters of single dendrimers. To make sure that the fluorescence is coming from dendrimers, fluorescence spectra were taken from 20 bright dots (figure 10B). Averaging these 20 spectra resulted in a spectrum resembling very well a solution spectrum in CHCl$_3$.
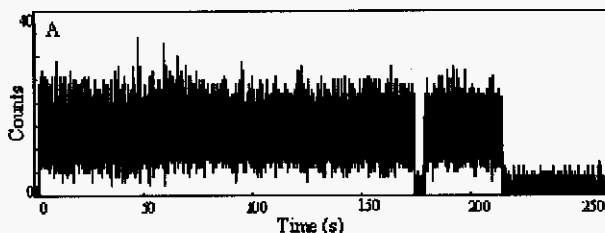

Figure 11. Emission transient observed from one single dendrimer

Figure 11 represents the emission transient of a *single macromolecule*, obtained by parking the laser beam on one of the bright spots from figure 10A. In the transient several typical single molecule features can be seen. First of all, the signal is quite noisy due to Poisson shot noise (and fluctuations of the laser power (10%)). Further, the emission intensity of the dendrimer goes 'off' at a certain moment and later on turns 'on' again. This switching to the 'off-state' could be attributed to crossing over to a low-emissive state (e.g. T$_1$. state), hence blocking the rapid cycling between S$_0$ and S$_1$. For the dendrimers studied, it must be noticed that switching is a rare event, indicating a very low probability of formation of the non-emitting state. Another explanation could be that the state crossing and a relaxation of this state to the ground state in the dendrimer molecule occurs on a much faster time scale than the one on which the experiment is performed (10 ms dwell time). The last typical feature is the sudden and discrete photobleaching of the single molecule leading to background level emission intensity.

Using an electro-optical modulator (EOM) in the excitation beam path, linear polarized light with a slowly rotating polarization direction (1 Hz modulation frequency) was produced. Two APD's (avalanche

photodiodes) and a polarizing beam splitter were placed into the detection path. From variations of the two detected intensities and from the phase shift of the signal with respect to the modulation, it was shown that the orientation of the absorption transition dipole of single dendrimer molecules in the polymer film changes in a time window of seconds. In this way we were also able to distinguish single molecules from small clusters.

Submolecularly resolved imaging of light induced reactions.

Since the first STM related publications of physisorbed monolayers on alkanes and long-chain alcohols (13) such self-organized monomolecular adlayers have been studied with STM for a broad range of compounds (14). Physisorbed monolayers of organic molecules at the liquid/graphite interface containing photoactive groups were recently reported (15) and the light induced cis-trans isomerization could be imaged with submolecular resolution (16,17). The photopolymerization of a physisorbed monolayer containing diacetylene moieties, self-assembled from solution at the liquid/graphite interface was recently reported (18).
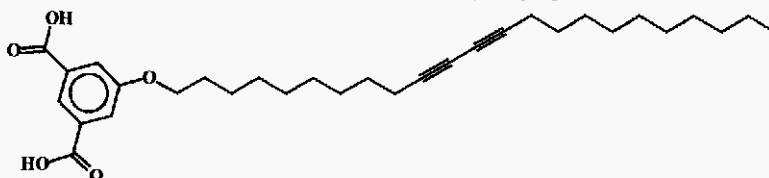

Figure 12. structure of ISAC$_9$(DIA)C$_{10}$

When a drop of the solution of ISAC$_9$(DIA)C$_{10}$ in 1-undecanol is applied to the graphite surface, a physisorbed monolayer is spontaneously formed at the liquid/graphite interface. Figure 13 A shows the image

Figure 13. A. An STM image of a physisorbed monolayer of ISAC$_9$(DIA)C$_{10}$ molecules from a solution in 1-undecanol, image size 12.7 x 12.7 nm^2. White corresponds to the highest and black to the lowest measured tunneling current in the image. Bias voltage and average tunneling current were -1.2 V and 1.0 nA, respectively. B. An STM image of a polymerized monolayer structure. White corresponds to the highest and black to the lowest measured tunneling current in the image. Image size: 10.8 x 10.8 nm^2. Bias voltage and average tunneling current were -0.5 V and 1.0 nA, respectively.

of the structure of such a monolayer observed with STM. The structure consists of lamellae of the ISAC$_9$(DIA)C$_{10}$ molecules (ISA figure 13A) alternated by lamellae consisting of solvent molecules (SOLV figure 13A). The distance from one ISA headgroup to the next one is 9.44 ± 0.09 Å. Comparison with the HOPG reference image (not shown), acquired immediately after the STM image of the physisorbed monolayer, shows that the alkyl chains of the ISAC$_9$(DIA)C$_{10}$ molecules are lying in the direction of one of the main graphite axes. The specific STM contrast in Figure 13 B is more indicative of a polydiacetylene, characterized by a sequence of double, single, triple and single bonds. The most important change in the monolayer structure with respect to the image in Figure 13A, however, is the change in the spacing between

the ISA headgroups. This repeating distance was determined to be 9.81 ± 0.05 Å, in contrast to the unpolymerized repeating distance of 9.44 ± 0.09 Å. The experimental value of 9.81 Å for the ISA headgroup distance is in perfect accordance with the value of 9.82 Å obtained in a model optimized for the polymer chain.

CONCLUSION

The results reported clearly illustrate the potentiality of coupling photochemistry or photophysics to space resolution. The ultimate challenge to couple submolecular resolution to femtosecond time resolution is for organic systems not achieved as yet but is now within reach. These methods further coupled to nanomanipulation visualized in real time will enable a new approach to nanoscience. This opens new research avenues in material and biosciences where photochemistry and photophysics will be a major research component.

References
(1) W. Verbouwe, M. Van der Auweraer, F.C. De Schryver, J. J. Piet, J.M. Warman *J.Am.Chem.Soc.*, **120**, 1319-1325 (1998).
(2) G. Schweitzer, L. Xu, B. Craig, F.C. De Schryver *Optics Communications*, **142**, 283-288. H.A.M. Biemans, A. Verhoeven, A.E. Rowan, A.P.H.J. Shenning, L. Latterini, J. Foekema, F.C. De Schryver, E.W. Meijer and R.J.M. Nolte, submitted. L. Latterini, G. Schweitzer, A.E. Rowan, E.W. Meijer, F.C. De Schryver and R.J.M.Nolte, in preparation (1997).
(3) S. De Backer, Y. Prinzie, W. Verheijen, M. Smet, K. Desmedt, W. Dehaen, F.C. De Schryver *J.Phys.Chem.*, in press (1998).
(4) G.J. Brakenhoff, P. Blom, P. Barends, *J. Microsc.*, **117**, 219 (1979).
(5) A.Ashkin, *Phys. Rev. Lett.*, **24**, 156, (1970).
(6) A. Ashkin, J.M. Dziedzic , *Appl. Phys. Lett.*, **19**, 283 (1971).
(7) A. Ashkin, J.M. Dziedzic, J.E. Björkholm, S. Chu, *Opt. Lett.*, **11**, 288 (1986).
(8) N. Kitamura, K. Sasaki, H. Misawa, H. Masuhara, In *Microchemistry: Spectroscopy and Chemistry in Small Domains*, H. Masuhara, F. C. De Schryver, N.Kitamura and N. Tamai, Ed.; North-Holland: Amsterdam, pp. 35. (1994)
(9) T. Gensch, J. Hofkens, J. van Stam, H. Faes, S. Creutz, K. Tsuda, R Jérôme, H Masuhara and F. C. De Schryver submitted
(10) J.Hofkens, L.Latterini, H.Faes,P.Vanoppen, K.Jeuris, S.De Feyter, J.Kerimo, P.F.Barbara , A. E. Rowan, R. J.M. Nolte and F.C.De Schryver ,*J.Phys.Chem.*, **101**, 10588-10598 (1997).
(11) L. Latterini, R. Blossey, J. Hofkens, P. Vanoppen, A. Rowan, R.J.M. Nolte, F.C. De Schryver. Submitted
(12) J. Hofkens, W. Verheijen, R. Shukla, W.Dehaen, F.C. De Schryver *Macromolecules*, in press (1998).
(13) a) G.C. McGonical, R.H. Bernhardt, D.J. Thomson, *Appl. Phys. Lett.*, **57**, 28-30 (1990); b) J.P. Rabe, S. Buchholz, *Science*, **253**, 424-427 (1991).
(14) D.M. Cyr, B. Venkataraman, G.W. Flynn, *Chem. Mater.*, **8**, 1600-1615 (1996).
(15) R. Heinz, A. Stabel, J.P. Rabe, G. Wegner, F.C. De Schryver, D. Corens, W. Dehaen, C. Süling, *Angew. Chem.*, **106**, 2154-2157 (1994); *Angew. Chem. Int. Ed. Engl.*, **33**, 2080-2083 (1994).
(16) P.C.M. Grim, P. Vanoppen, M. Rücker, S. De Feyter, G. Moessner, S. Valiyaveettil, K. Müllen, F.C. De Schryver, *J. Vac. Sci. Technol. B*, **15**, 1419-1424 (1997).
(17) P. Vanoppen, P.C.M. Grim, M. Rücker, S. De Feyter, G. Moessner, S. Valiyaveettil, K. Müllen, F.C. De Schryver, *J. Phys. Chem.*, **100**, 19636-19641 (1996).
(18) P.C.M. Grim, S. De Feyter, A. Gesquière, P. Vanoppen, M. Rücker, S. Valiyaveettil, C. Moessner, K. Müllen, F.C. De Schryver, *Angewandte Chemie*, **36**, 2601-2603 (1997).